Development of an atmospheric-pressure homogeneous and cold Ar / O 2 plasma source operating in glow discharge

Shou-Zhe Li, Qi Wu, Jialiang Zhang, Dezhen Wang, and Han S. Uhm

Citation: Physics of Plasmas (1994-present) **17**, 063506 (2010); doi: 10.1063/1.3447877
View online: http://dx.doi.org/10.1063/1.3447877
View Table of Contents: http://scitation.aip.org/content/aip/journal/pop/17/6?ver=pdfcov
Published by the AIP Publishing

Development of an atmospheric-pressure homogeneous and cold Ar/O_2 plasma source operating in glow discharge

Shou-Zhe Li,[1,a] Qi Wu,[1] Jialiang Zhang,[1] Dezhen Wang,[1] and Han S. Uhm[2]
[1]*Key Laboratory of Materials Modification by Laser, Ion and Electron Beams, Ministry of Education, School of Physics and Optoelectronic Technology, Dalian University of Technology, Dalian 116023, China*
[2]*Kwangwoon Academy of Advanced Studies, Kwangwoon University, 447-1 Wolgye-dong, Nowon-gu, Seoul 137-701, Republic of Korea*

(Received 8 February 2010; accepted 3 May 2010; published online 23 June 2010)

An atmospheric-pressure Ar/O_2 glow discharge is generated in a parallel bare metal plate reactor with a radio-frequency power supply by introducing a dielectric strip in the inlet of the gas flow. The role of the dielectric strip is discussed experimentally. The allowable oxygen-to-argon ratio reaches 1.0 vol % and the generated Ar/O_2 plasma discharge is characterized by a low gas temperature and good spatial homogeneity, implying its feasible application as a type of material treatment for a large-area surface, as illustrated experimentally by the ashing of carbon black. © *2010 American Institute of Physics*. [doi:10.1063/1.3447877]

I. INTRODUCTION

Atmospheric-pressure glow discharge (APGD) is typically used in open ambient environments to reduce operating cost through the elimination of the need for a vacuum system. This type of plasma discharge provides numerous advantages in applications to surface modification, material synthesis, and biological decontamination,[1,2] and it also presents challenge in its igniting, maintaining, stability controlling, and widening the physical and chemical operating window.[3–10] Capacitively coupled radio-frequency (rf) discharge is commonly employed to generate homogeneous APGD with helium as a carrier gas.[3–5] Considering the cost in terms of gas consumption, much attention has been paid recently to the replacement of helium with argon due to the low price of argon. In these efforts, a dielectric barrier discharge (DBD) is adopted to enlarge the discharge gap between the electrodes and chemical operating window.[6–9] However, with regard to the use of argon, the dielectric layers in the DBD prevents the thermal release to electrodes and the thermal conductivity of the argon discharge is nearly ten times less than that of a helium discharge, resulting that the discharge characteristics, such as the homogeneity and the physical operating window, are severely deteriorated due to heat accumulation. Therefore, configuration of a bare metal electrode must be done to increase the thermal release, as heat removal by conduction through bare metal electrodes is more effective than convective cooling through an increase in the flow rate through a large discharge zone.[10] Unfortunately, in argon rf-APGD in a bare metal electrode configuration, it is difficult to mix an active gas such as oxygen into a carrier gas, especially argon, at a certain ratio and maintain good stability. In this context, we propose a scheme to obtain a homogeneous and cold Ar/O_2 APGD through the introduction of a dielectric strip between bare metal electrodes. This approach enhances the local electric field in the gas inlet while inhibiting the occurrence of arcing where the electric field is the strongest. It was found that the threshold of the dielectric strip plays an important role in augmenting the mixture ratio of oxygen in an argon rf-APGD while suppressing the instability, maintaining good homogeneity, and widening the operating window. Furthermore, an ashing application is demonstrated in which carbon black is removed with the generated Ar/O_2 APGD.[2]

II. EXPERIMENTAL SETUP

The experimental configuration is illustrated in Fig. 1(a), where the bare metal electrodes are made of stainless steel and the dielectric strip is made of Teflon. The size parameters are labeled in units of millimeters in Fig. 1(b), where the dielectric strip partitions the plasma source into three regions: S1, S2, and S3. Both electrodes are cooled by circulated water. A rf power supply is connected to the upper electrode through a manual matching *L*-type network, and the bottom electrode is grounded. The voltage and current are recorded by a Tektronix® oscilloscope (TDS 220, 100 MHz) using a high-voltage probe (P6015A) and a Pearson current-coil (Pearson 4100). The optical emission of the plasma discharge is transmitted through an optical fiber and is recorded by a spectrometer (Acton Research SpectraPro–2500i) with 1200 grooves/mm gratings and an entrance slit of 50 μm. To measure the optical emission from the plasma source inside, the head of the optical fiber is located perpendicularly to the side view window in the middle of region S1 and the effluent of the plasma discharge is measured near the outlet of the plasma source.

III. EXPERIMENTAL RESULTS AND DISCUSSIONS

The plasma discharge was struck in Ar (99.995%) and the oxygen gas was then fed into argon plasma at a certain volume ratio. It is notable that the discharge occurs only in region S1 at a gas flow rate of 28 l/min, despite the fact that the input power is raised to such a value that the α mode transmits to the γ mode. We attribute this to pressure dis-

[a]Electronic mail: lisz@dlut.edu.cn.

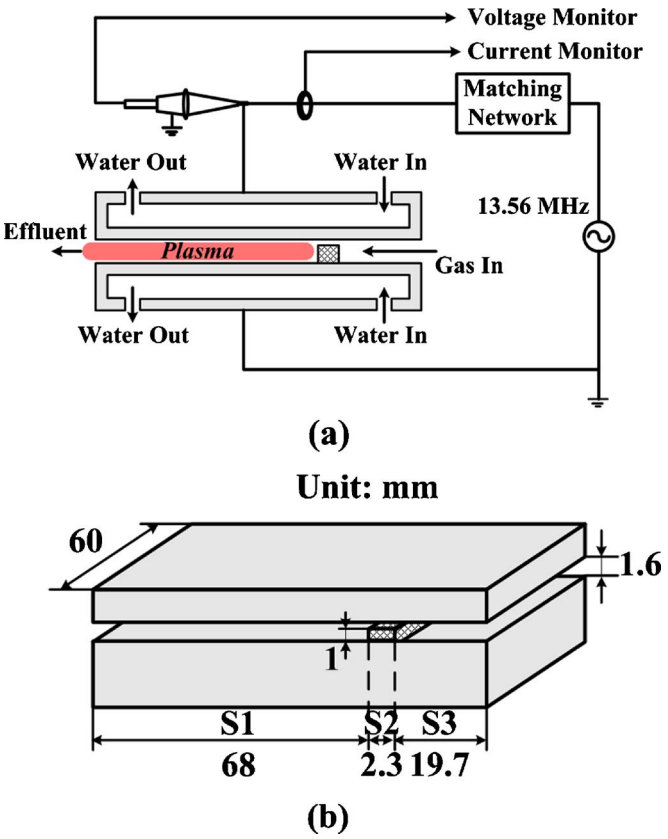

FIG. 1. (Color online) (a) Schematic of the experimental setup and (b) sketch of the reactor with size labeled in units of mm.

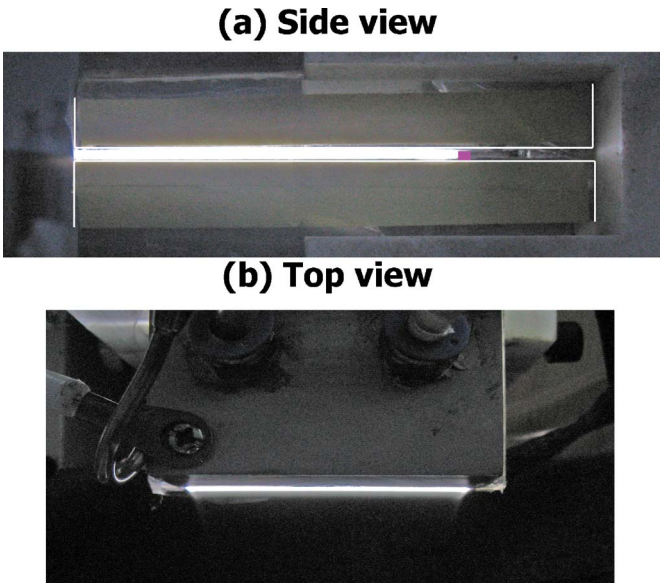

FIG. 2. (Color online) Images of the plasma discharge from (a) the side and (b) the top at a total flow rate of 28 l/min, at an oxygen-to-argon ratio of 0.6 vol %, and an input power of 200 W, where the purple block represents the dielectric strip on the bottom electrode.

crepancies in regions S1, S2, and S3. To feed gas into the discharge region from S3 to S1 at a certain flow rate, there must be a pressure difference from the inlet (region S3) to the outlet (region S1); it was experimentally shown that the discharge occurs in both the S1 and S3 regions in static argon. In addition, the gap of region S2 must be narrow enough so that the discharge in region S1 cannot spread into region S3 with input power increasing. It is experimentally found that the gap should be smaller than 0.7 mm. In the present case, it was set at 0.6 mm. The mechanism of electrical breakdown in rf discharge is closely related to electrode separation. It is known that when discharge occurs in the narrow electrode separation, the loss rate of electrons to the electrode is the dominant factor and the surface effects, particularly electron-induced secondary emission, play an important role in determining the breakdown characteristics.[11] In this experiment, it was found that when the electrode separation distance is less than 0.7 mm, the breakdown occurs at a higher applied voltage with the separation distance reducing further and the electric discharge directly transmits into arcing. On the contrary, when a separation distance is greater than 2.4 mm, the product of p (gas pressure) and d (distance of electrode separation) exceeds the critical value $(pd)_{cr}$ of argon and the discharge directly evolves into a γ discharge after electrical breakdown.[12] Thus, we set the electrode separation in section S1 to be 1.6 mm in the experiment to excite the plasma discharge into the glow state in an α mode at a lower applied voltage; at the same time, such an applied voltage is too low to ignite the electrical discharge in S2 at an electrode separation distance of 0.6 mm. The alteration of the dielectric-strip position on the electrode influences only the tuning parameters in achieving good matching in a matching network, as regions S2 and S3, without the occurrence of a discharge, acts as a capacitor in a parallel connection with region S1, the capacitance value of which is determined by the areas of regions S2 and S3, that is, the wideness and location of the dielectric strip. In addition, the introduction of a dielectric strip is very important when feeding oxygen gas into an Ar plasma discharge in that the maximum oxygen-to-argon ratio is allowed to approach 1.0 vol % while maintaining a stable Ar/O_2 plasma discharge. Without it, the oxygen-to-argon ratio cannot be allowed to exceed 0.25 vol %, which greatly restricts its potential application owing to its narrow chemical operating window. We know that the local electric field in narrow region S2 is strengthened compared with regions S1 and S3, especially around the corners of the dielectric strip, where the fed oxygen molecules are pre-excited by electrons diffusing from region S1 upstream, so that the molecules populate in numerous excited states, especially metastable states. The excitation of oxygen molecules weakens the electronegative properties and the involvement of the excited molecules, especially those in the metastable state such as $O_2(a\ ^1\Delta_g)$, in the Ar/O_2 plasma discharge imposes appreciable influences on the particle balance with respect to the electron production and loss, thereby providing the benefit of maintaining the plasma. The use of a dielectric material instead of metal in region S2 prevents arcing due to the strong electrical field at a high input power, thereby further enlarging its operating window. Typical images of the rf Ar/O_2 APGD operating in α mode at a total gas flow rate of 28 l/min, an oxygen-to-argon ratio of 0.6 vol %, and an input power of 200 W as taken with a Canon PowerShot A720 camera with an exposure time of 125 ms are shown in Fig. 2. These are a side

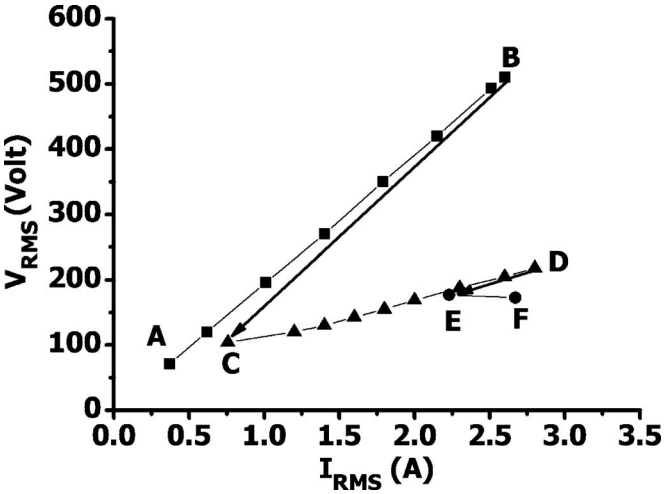

FIG. 3. Plot of the voltage vs the current in the rms for argon discharge at a total flow rate of 28 l/min.

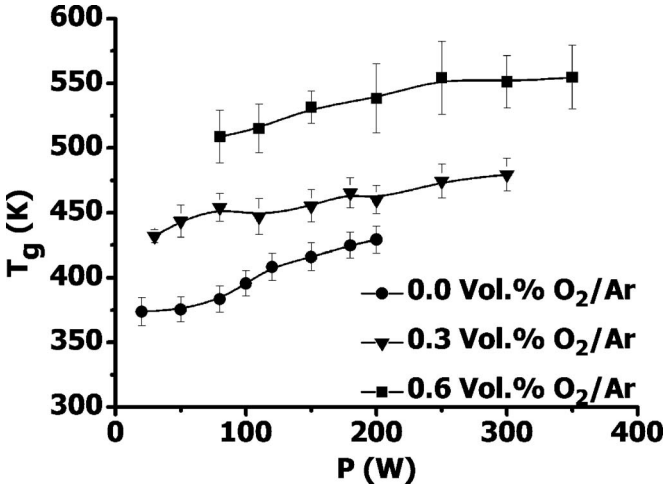

FIG. 5. Plot of the gas temperature T_g of the plasma in the reactor vs the input power for oxygen-to-argon ratios of 0.0 vol % (circular), 0.3 vol % (triangular), and 0.6 vol % (rectangular) at a total flow rate of 28 l/min.

view of the reactor through a quartz window in Fig. 2(a) and a top view of the plasma effluent in Fig. 2(b).

Figure 3 illustrates the current-voltage characteristic (CVC) curve when the input power is raised gradually in argon at a gas flow rate of 28 l/min. An electrical breakdown occurs at point B, the voltage in the root mean square (rms) drops from 510 to 104 V, and the total current is dominated by the conduction current in glow discharge region CD in α mode. With further increases in the input power, point D jumps to E in the CVC curve. At the same time, the contracted filaments emerge in the homogeneous glow background in region EF. This is ascribed to the coexistence of the α and γ modes. Control of the glow discharge in the α mode is important to obtain homogeneous and low-temperature plasma. The CVC curves were recorded in rms values in the glow discharge region at oxygen-to-argon ratios of 0.3 and 0.6 vol %, as shown in Fig. 4 together with the argon CVC curve for comparison at identical total gas flow rates of 28 l/min. It was found that each of the three CVC curves consists of two segments connected at points O, P, and Q, respectively, each varying almost linearly at different slopes with respect to two segments. The low current segment corresponds to a normal discharge in which the plasma discharge covers the electrode partially, dependent of the input power. The high current segment is associated with an abnormal discharge, where the electrodes are entirely filled and the brightness of the plasma discharge is enhanced as the input power increases. The oxygen is electronegative gas and the loss of electrons due to diffusion and attachment to oxygen molecules in O_2/Ar plasma requires the electrical field strength in the plasma to be higher than in argon plasma so as to produce enough electrons to maintain the plasma discharge. As the number of additional oxygen molecules increases, a progressively higher electrical field is required. The Joule heat release in the plasma discharge weighs much more with regard to the power consumption at atmospheric pressure due to the frequent collisions between particles.[13] The variation in the Joule heat versus the input power was monitored here by measuring the gas temperature in the reactor by means of optical emission spectroscopy (OES). When argon is used as the carrier gas, the dissociation of the water molecules existing in the argon gas gives rise to a hydroxyl (OH) molecular band ($A\ ^2\Sigma^+$, $\nu=0 \rightarrow X\ ^2\Pi$, $\nu'=0$, 306–310 nm) according to an OES analysis. In a previous study, it was found that good identification of the spectrum is suitable for the exploitation of the Boltzmann plot method to determine the gas temperature.[14] Therefore, the gas temperatures inside the plasma source versus the input power with respect to oxygen-to-argon ratios of 0.0, 0.3, and 0.6 vol % were determined. These are plotted in Fig. 5. The tendency of the variation shows that the gas temperature increases with the input power, as expected. It was remarkable to observe that even if the input power was augmented from several tens to several hundreds of watts, the gas temperature increased to not more than 100 K. It is the heat release by thermal conduction through the metal electrodes cooled by circulated water that comes into operation effectively to re-

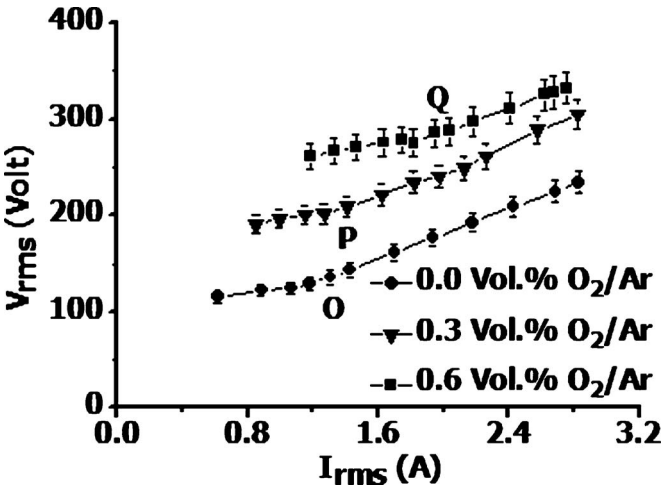

FIG. 4. Plot of the curves of the voltage vs the current in the rms in glow discharge regions for oxygen-to-argon ratios of 0.0 vol % (circular), 0.3 vol % (triangular), and 0.6 vol % (rectangular) at a total gas flow rate of 28 l/min.

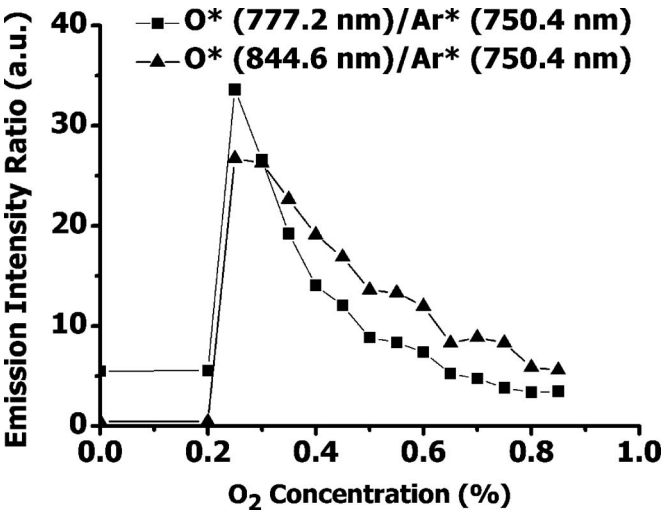

FIG. 6. Emission intensity ratios of $O^*(844.6\ nm)/Ar^*(750.4\ nm)$ and $O^*(777.4\ nm)/Ar^*(750.4\ nm)$ as a function of the O_2 concentration at a total gas flow rate of 28 l/min and an input power of 150 W.

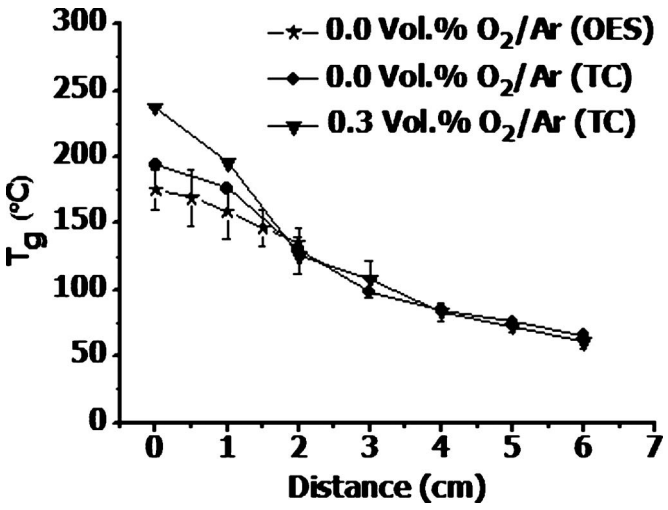

FIG. 7. The distribution of the gas temperature T_g of the effluent outside the reactor vs the distance along the gas flowing direction at a total flow rate of 28 l/min and an input power of 150 W with respect to the oxygen-to-argon ratio at 0.0 vol % by OES (star), 0.0 vol % by TC (circular), and 0.3 vol % (triangular) by TC.

duce the temperature, whereby the thermal instability is to be restrained effectively compared to a conventional rf DBD and a cold plasma discharge is obtained.

With regard to the Ar/O_2 plasma discharge generated at atmospheric pressure, it is also remarkable that the maximum oxygen-to-argon ratio could approach 1.0 vol % in this case and that the discharge keeps good stability, which greatly improves its performance compared with a conventional plasma reactor consisting of parallel metal plate electrodes. The concentration of the atomic oxygen generated in the plasma discharge is closely related to improvements in the operating efficiency and treatment effect in various potential applications. The oxygen radical density can be determined actinometrically using the emission of atomic oxygen at the two different wavelengths of $\lambda=777.4$ nm ($3p^5P\rightarrow 3s^5S$ transition) and $\lambda=844.6$ nm ($3p^3P\rightarrow 3s^3S$ transition), each ratioed to the argon emission at a wavelength of $\lambda'=750.4$ nm to obtain a pair of the intensity ratios.[15] Figure 6 illustrates the variation tendency of $O^*(844.6\ nm)/Ar^*(750.4\ nm)$ and $O^*(777.4\ nm)/Ar^*(750.4\ nm)$ emission intensity ratios as a function of the O_2 concentration from 0 to 0.9 vol % in argon at an input power of 150 W and a total gas flow rate of 28 l/min. Additionally, the two curves follow the coincident variation tendency and reach their maximum at an identical concentration ratio in the vicinity of 0.3 vol %, where most oxygen radicals are produced according to the actinometrical diagnosis. We attribute this to the competition occurring during the generation of O atoms by the electron impact dissociation processes, in which on one hand the reaction rates are proportional to the O_2 concentration and the electron density, and on the other hand the electron density decays as the O_2 concentration increases due to the electron attachment process to oxygen.

The gas temperature of the plasma-discharge effluent is another consideration for application as a surface treatment. As the ambient influence in the OES analysis of the detected hydroxyl (OH) molecular band outside the reactor becomes appreciable with the distance from the outlet of the plasma source, a thermocouple (TC) was used to measure the gas temperature outside the reactor without disturbing the plasma discharge in the reactor. The gas temperature measured with the TC was examined by comparing the results from the OES analysis to those with the TC in an argon discharge and the consistent experimental data shown in Fig. 7 validate its employment in the temperature measurement. The measured gas temperature outside the reactor is plotted with respect to the distance from the slot outlet of the plasma source in Fig. 7 for the two cases of oxygen-to-argon ratios of 0.0 and 0.3 vol % at a total gas flow rate of 28 l/min and an input power of 150 W. The gas temperature decreases with the distance, as expected. In the distance range from 1 to 2 cm, the gas temperature is brought down below 125 °C. Hence, it is possible to treat some temperature-sensitive materials by adjusting the distance between the sample and the outlet of the plasma source within the coverage of the effluent with sufficient concentration of the oxygen radicals, such as the long lifetime metastable particles. In addition, the spatial homogeneity of the effluent along the slot of the outlet of the plasma source is important for practical applications involving a large-area surface treatment. The spatial homogeneity is commonly defined as $1-(max-min)/(max+min)$ in percent and is evaluated with maximum and minimum values of the spatial distribution of the line-integrated total emission intensity of the Ar I or the gas temperature.[8] The closer the value approaches the unity, the better spatial homogeneity is achieved. In the present case, we measured the spatial distribution of the gas temperature of the effluent along the slot of the outlet of the plasma source. We therefore estimated the spatial homogeneity to be 97.7% according to above definition at a total gas flow rate of 28 l/min and an input power of 200 W in an argon discharge, presenting good homogeneity.

To demonstrate the practical performance of the generated Ar/O_2 APGD, we exploited it in the ashing of carbon black. Carbon black was produced and uniformly spread on a

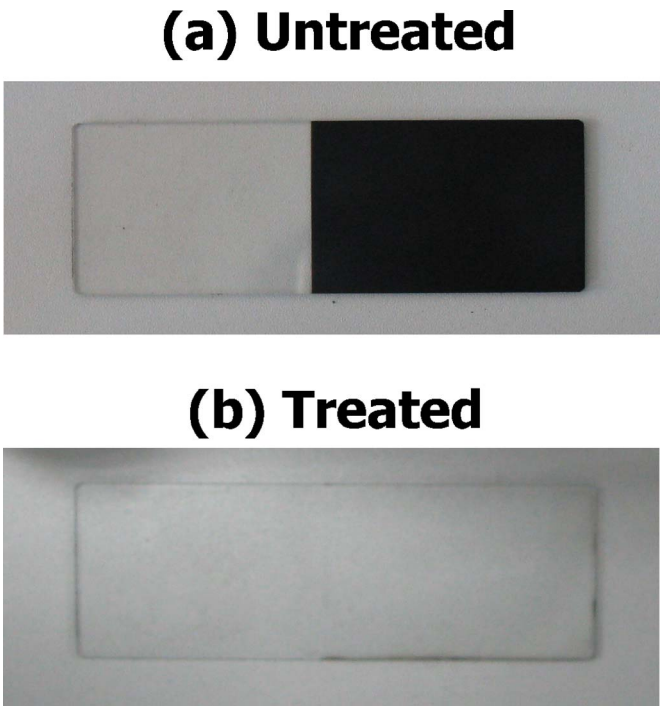

FIG. 8. (Color online) Images of (a) a prepared slide glass with carbon black and (b) a treated sample at a total gas flow rate of 21 l/min, an input power of 150 W, and an oxygen-to-argon ratio of 0.3 vol % at a treatment time of 3.5 min.

slide glass at a mass density of 0.828 mg cm^{-2}. The plasma effluent was generated at an input power of 150 W, a total gas flow rate of approximately 21 l/min, and an oxygen-to-argon ratio fixed at 0.3 vol %. The slide glass was placed under the effluent at a distance of 0.5 cm from the slot outlet of the plasma source. In 3.5 min, the carbon black on the slide glass was completely removed by an oxidation process between the free carbon and the produced atomic oxygen.[2] The ashing rate was approximately 0.237 mg cm^{-2} min^{-1}. The image shown in Fig. 8(a) exhibits the prepared sample while that in Fig. 8(b) shows the result after the treatment to present a visual impression by comparison. In the experiment, it was also verified that carbon black produced as such could not be eliminated by pure argon plasma effluent, even at an input power greater than 200 W and even when using a much higher gas flow. This confirms the role of oxygen radicals generated in the Ar/O_2 APGD in an ashing test.

IV. CONCLUSION

In summary, this study proposed a scheme to generate a homogeneous and cold Ar/O_2 APGD at atmospheric pressure with the use of a rf power supply operating at 13.56 MHz. Its characteristics were investigated by measuring the CVC curves, gas temperature dependence on the input power, and the temperature distribution and spatial homogeneity of the effluent. Moreover, it was found that there exists an optimal oxygen-to-argon ratio at which most oxygen radicals are produced. To demonstrate the feasibility of the proposed method, a practical treatment of carbon black by Ar/O_2 APGD was successfully carried out.

ACKNOWLEDGMENTS

This work was supported by the National Natural Science Foundation of China under Grant Nos. 50777004, 10775026, and 10675028 and by SRF for ROCS, SEM under Grant No. 20071108.

[1] K. H. Becker, U. Kogelschatz, K. H. Schoenbach, and R. J. Barker, *Non-equilibrium Air Plasmas at Atmospheric Pressure* (IOP, Bristol, 2005).
[2] A. Grill, *Cold Plasma in Materials Fabrication from Fundamentals to Applications* (IEEE, New York, 1994).
[3] J. Park, I. Henins, H. W. Herrmann, and G. S. Selwyn, J. Appl. Phys. **89**, 20 (2001).
[4] S. Reuter, K. Niemi, V. Schulz-von der Gathen, and H. F. Döbele, Plasma Sources Sci. Technol. **18**, 015006 (2009).
[5] J. J. Shi and M. G. Kong, Appl. Phys. Lett. **90**, 101502 (2007).
[6] B. Li, Q. Chen, and Z. W. Liu, Appl. Phys. Lett. **96**, 041502 (2010).
[7] A. P. Yalin, A. Rahman, C. Moore, R. Rahul, O. Stan, Z. Yu, and G. J. Collins, IEEE Trans. Plasma Sci. **33**, 562 (2005).
[8] S. Y. Moon, W. Choe, and B. K. Kang, Appl. Phys. Lett. **84**, 188 (2004).
[9] H.-P. Li, G. Li, and S. Wang, IEEE Trans. Plasma Sci. **36**, 1418 (2008).
[10] J.-P. Lim, H. S. Uhm, and S.-Z. Li, Appl. Phys. Lett. **90**, 051504 (2007).
[11] H. B. Smith, C. Charles, and R. W. Boswell, Phys. Plasmas **10**, 875 (2003).
[12] Y. P. Raizer, M. N. Shneider, and N. A. Yatsenko, *Radio-Frequency Capacitive Discharges* (CRC, Boca Raton, 1995).
[13] N. Moravej, S. E. Babayan, G. R. Nowling, X. Yang, and R. F. Hicks, Plasma Sources Sci. Technol. **13**, 8 (2004).
[14] S.-Z. Li, W.-T. Huang, and D. Wang, Phys. Plasmas **16**, 093501 (2009).
[15] M. A. Lieberman and A. J. Lichtenberg, *Principles of Plasma Discharges and Materials Processing* (Wiley, New York, 1994).